Wood Science and Technology 31 (1997) 415–422 © Springer-Verlag 1997

An experimental assessment of driving forces for drying in hardwoods

T. A. G. Langrish, N. Bohm

Summary An investigation has been carried out into whether the internal moisture movement inside Australian hardwood timber is best described by a diffusion model with driving forces based on gradients in moisture content or in partial pressure of water vapour. Experimental data from two sets of drying schedules applied to timber from three species of Australian hardwoods (yellow stringybark, spotted gum and ironbark) reported in Langrish et al. (1997) have been used to assess the use of the two driving forces, and the standard error has been used as the criterion for goodness of fit. Moisture-content driving forces have fitted the data better than a model based on vapour-pressure driving forces alone. The use of moisture-content driving forces with diffusion parameters obtained from data from one drying schedule is also better in predicting the drying behaviour with another schedule than vapour-pressure driving forces for yellow stringybark and ironbark. These results may be due to the complexity of the moisture-movement process through timber, with more than one moisture-transport mechanism being active, so that the use of only one driving force for moisture movement is at best only an approximation to the true behaviour.

Symbols

- D diffusion coefficient, $m^2\ s^{-1}$ (moisture-content gradient), $m^3\ s\ kg^{-1}$ (vapour-pressure gradient)
- D_e activation energy, K
- D_r pre-exponential factor $m^2\ s^{-1}$ (moisture-content gradient), $m^3 s\ kg^{-1}$ (vapour-pressure gradient)
- J mass flux of water divided by density, $m\ s^{-1}$
- t time, s
- x position, m
- X moisture content, $kg\ kg^{-1}$

Introduction

A knowledge of the mechanisms of moisture movement in timber is relevant to predicting the rate at which boards of timber dry and also to predicting the stresses

Received 22 September 1996

T. A. G. Langrish, N. Bohm
Department of Chemical Engineering,
University of Sydney, N.S.W. 2006, Australia

This work has been supported by the Australian Research Council, the Ian Potter and George Alexander Foundations, and The University of Sydney Research Grant Scheme.

which develop in timber during drying. These stresses arise because of differential shrinkage between the surface and the center of timber boards and may be sufficient to cause the timber of crack, leading to degrade in the board quality.

Recently, Bramhall (1995) has discussed mechanisms for moisture movement through timber and suggested that using a driving force based on gradients in the partial pressure of water vapour inside boards to predict drying rates has a more fundamental basis than using gradients in moisture contents. However, Stanish et al. (1986) have found that there is a number of mechanisms for the movement of moisture inside timber and other materials with complex porous structures. These mechanisms include the movement of water vapour, liquid water and water which is bound to the cell structure and, in the case of water vapour and bound water, these may occur simultaneously. For the drying of a softwood timber (*Pinus radiata*), Pang et al. (1994) have found that a drying model based on these simultaneous physical mechanisms predicts the temperature gradients inside timber well as it dries.

For the optimisation of timber drying schedules, as reported recently by Langrish et al. (1997), the use of the simplest reasonable drying model has a considerable advantage in terms of reducing the computational time. For Australian hardwood timbers, as studied in that work, Wu (1989) has found that a drying model based on gradients in moisture concentration (which is proportional to the moisture content) can be used to fit both the moisture-content gradients and the overall drying rates adequately. This approach has been used to produce the optimised schedules reported in Langrish et al. (1997). These schedules have been found to give better timber quality and shorter drying times compared with the conventional drying schedules suggested by Campbell (1980) (referred to here as C.S.I.R.O. schedules). The drying rate data from these two schedules are used in this work to assess whether a drying model based on vapour-pressure driving forces describes the drying behaviour better than the previously-used model based on moisture-content driving forces.

Given the complexity of the movement of moisture through timber, there is no assurance that vapour-pressure driving forces (on their own) will fit the drying behaviour better than moisture-content driving forces. The two driving forces are not exactly equivalent, since the partial pressure of water vapour is not proportional to the moisture content according to the sorption isotherm of Simpson and Rosen (1981).

The two driving forces and their relationship with the moisture movement flux will be outlined briefly first, before their use for fitting the drying data from both C.S.I.R.O. and optimised schedules is compared. The experimental equipment and method are described in Langrish et al. (1997), and these descriptions will not be repeated here.

Theory

Since timber boards are usually much longer and wider than they are thick, this three-dimensional transport problem can be reduced to a single dimension with little loss of accuracy. With this assumption made, Doe et al. (1994) have suggested that moisture transport within Australian hardwoods may be adequately described by a simple diffusion model (Fick's Second Law):

$$\frac{\partial X}{\partial t} = \frac{\partial}{\partial x}(J) \qquad (1)$$

Here X is the moisture content, t is time, x is the position within the timber board, and J is the flux of water vapour inside the timber. The diffusion coefficient, D, is modelled as a temperature-dependent parameter (as in Doe et al., 1994):-

$$D = D_r e^{\frac{-D_e}{T}} \quad . \tag{2}$$

If the gradient in the moisture content is assumed to be the driving force for moisture movement, the flux of water vapour is given by the following equation:-

$$J = D\frac{\partial X}{\partial x} \tag{3}$$

If, however, the flux is driven by gradients in the partial pressure of water vapour (p_v), then the following equation for the flux is more appropriate:-

$$J = D\frac{\partial p_v}{\partial x} \tag{4}$$

Where the vapour pressure (p_v) has been obtained from the correlation of Simpson and Rosen (1981).

The rest of the model, including the energy transport model, the boundary and initial conditions, and the solution method, are all described in Langrish *et al.* (1997) and will not be repeated here.

The first method used here to assess the applicability of each driving force has been to evaluate the degree of fit which can be achieved using each driving force (moisture content and vapour pressure) to fit the moisture-content data for each species. The degree of fit has been quantified using the standard error, defined as:-

$$\text{Standard error} = \frac{\sqrt{\sum (Y_{\text{Model}} - Y_{\text{Expt}})^2}}{(n-1)} \tag{5}$$

where Y_{Model} is the fitted moisture content, Y_{Expt} is the experimentally-measured moisture content, and the sum is taken over all the n data points from each schedule. A low standard error for one driving force relative to the other suggests that the former is more appropriate for modelling the drying process than the latter.

The second method for assessing the relative applicability of the two driving forces has been to evaluate how well each of these approaches (moisture content and vapour pressure) extrapolate to different drying conditions. In this method, the parameters in the diffusion model were fitted to the drying data (moisture contents against time) from the C.S.I.R.O. schedule using each of the driving forces (in turn). Using these fitted parameters and each driving force, the drying curves were predicted for the optimised schedule, and compared with the experimentally-observed values. Again, the criterion used to determine the degree of fit was the standard error, as defined above.

The results of applying these two methods will now be presented.

Results

The drying schedules and graphical presentations of the degree of fit for each schedule are shown in Figures 1, 2 and 3 for each species of timber.

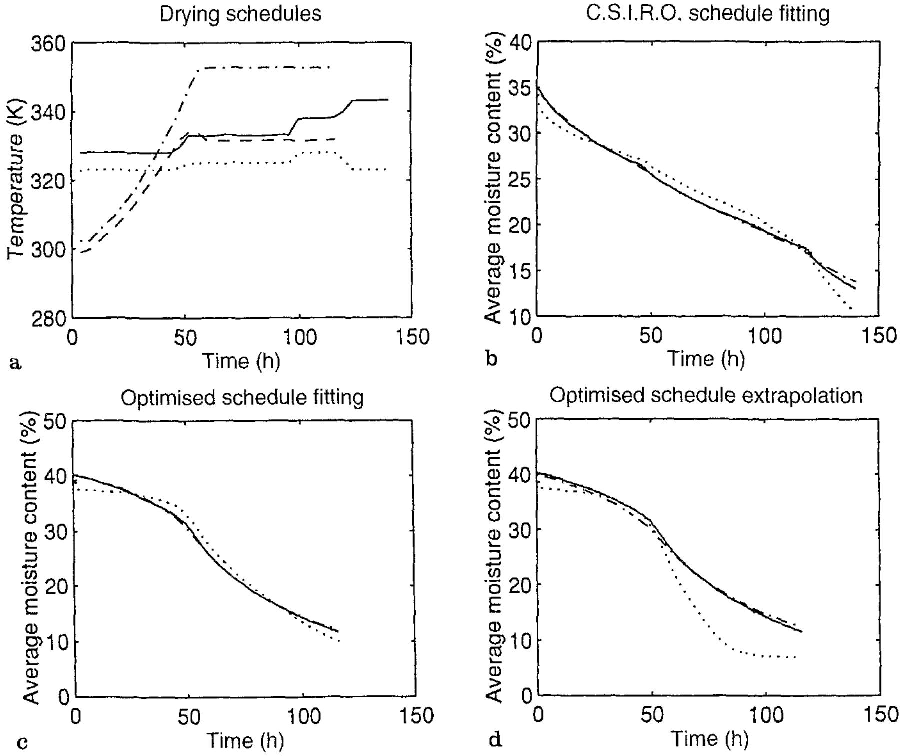

Fig. 1. Drying schedules, fitted and measured drying curves for yellow stringybark (**a**) drying schedules, — dry-bulb temperature, C.S.I.R.O. schedule, ···· wet-bulb temperature, C.S.I.R.O. schedule, -·- dry-bulb temperature, optimised schedule, - - wet-bulb temperature, optimised schedule, (**b**) fitting of experimental data from the C.S.I.R.O. schedule, — experimental data, ···· vapour-pressure driving forces, -·- moisture-content driving forces, (**c**) fitting of experimental data from the optimised schedule (same key as (b)), (**d**) extrapolation of parameters from the C.S.I.R.O. schedule to the optimised schedule (same key as (b))

For each driving force and drying schedule, the fitted diffusion parameters (equation 2) are given in Table 1, and the standard errors (equation 5) are presented in Table 2.

Discussion

Fitted diffusion parameters

For a driving force based on moisture-content gradients, the fitted activation energies (D_e) for the C.S.I.R.O. schedules (3700–3800 K) are similar to that reported by Wu (1989) for Tasmanian eucalypt timber of 3800 K (Table 1). The drying temperatures used by Wu (1989) were lower (less than 40 °C) than those used in the schedules recommended by C.S.I.R.O. here (under 70 °C). This result suggests that the diffusion behaviour of the timber is similar at 70 °C to that at 40 °C, and the activation energy for moisture movement through cellulose is expected to be virtually constant and independent of timber type. The fitted reference diffusuon coefficients (D_r) are expected to be related to the tortuosity of the timber structure. Without carrying out micrographs of the different timbers,

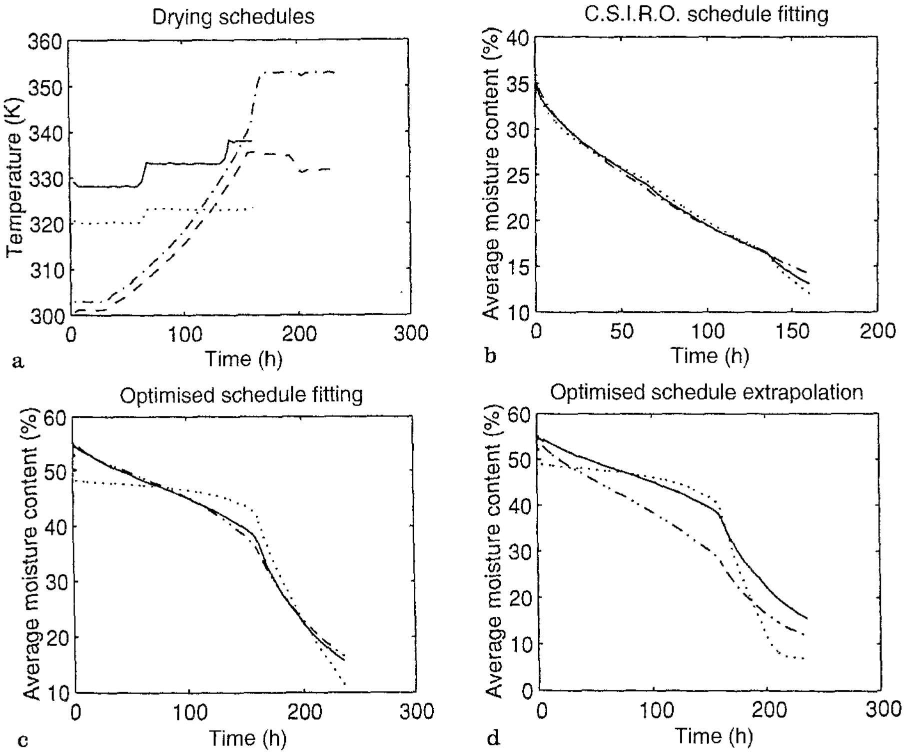

Fig. 2. Drying schedules, fitted and measured drying curves for spotted gum (same key as Fig. 1)

it is difficult to assess the significance of the variations seen here, except to say that the large variation between species has been reported in other studies.

For the generally higher temperatures used in the optimised schedules (up to 80 °C), the fitted activation energies (4300–5200 K) are higher and vary more widely than those for the C.S.I.R.O. schedules, while the fitted reference diffusion coefficients are lower. Table 2 shows that the fit between the model and the model predictions (with different diffusion parameters) is similar. The differences between the fitted diffusion parameters and those obtained from the C.S.I.R.O. model are large; an order of magnitude in the case of the reference diffusion coefficients, and over 50% for the activation energies. These differences suggest that the model using moisture-content driving forces may be less appropriate at relatively high temperatures, although the fit obtained using this driving force is better for both schedules than that obtained using vapour-pressure driving forces. However, the model based on moisture-content driving forces and the parameters obtained by fitting the model to the data from the C.S.I.R.O. schedules extrapolates the drying behaviour to the conditions used in the optimised schedules better, in general, than the model using vapour-pressure driving forces, as will be discussed further in the following section.

For the model based on vapour-pressure driving forces, the fitted diffusion parameters for the C.S.I.R.O. and optimised schedules are more similar than those for the model based on moisture-content driving forces. Nevertheless, there are still significant differences between the parameters estimated from the data of the

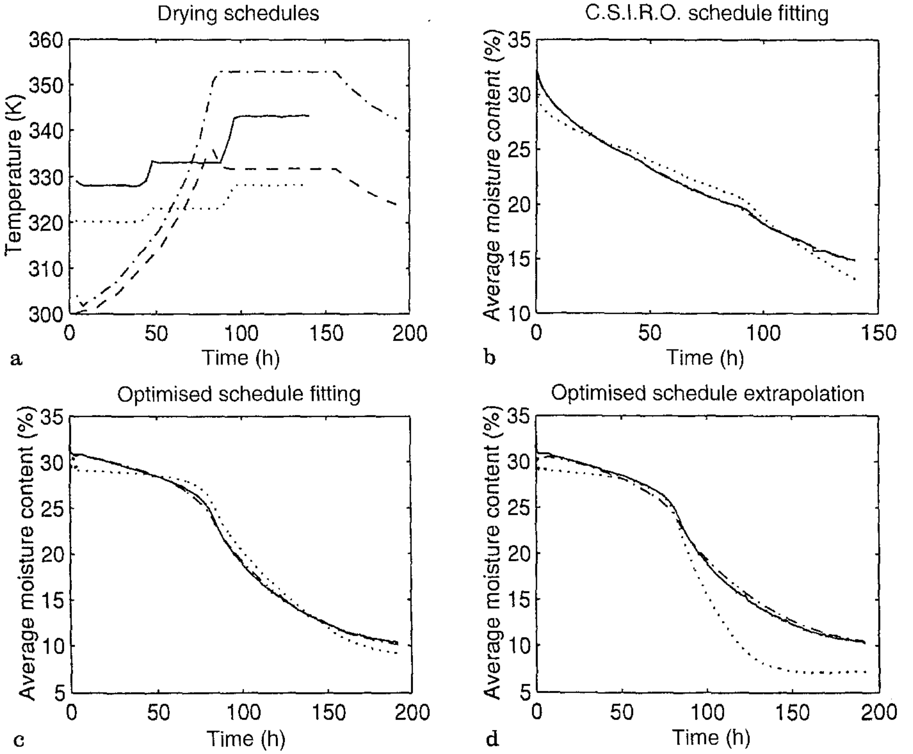

Fig. 3. Drying schedules, fitted and measured drying curves for ironbark (same key as Fig. 1)

two schedules, and the fit of the model to the data is worse for vapour-pressure driving forces than that for moisture-content driving forces.

Fit of the drying models to the experimental data

When fitting the two models to the experimental data, Table 2 shows that the fit is always better for that using moisture-content driving forces than for vapour-

Table 1. Fitted diffusion parameters

		Yellow Stringybark	Spotted Gum	Ironbark
Moisture-content driving forces				
C.S.I.R.O.	D_r (m^2 s^{-1})	6.65×10^{-5}	5.79×10^{-5}	4.66×10^{-5}
schedule	D_e (K)	3787	3770	3777
Optimised	D_r (m^2 s^{-1})	7.97×10^{-4}	2.25×10^{-4}	2.29×10^{-4}
schedule	D_e (K)	4633	5162	4308
Vapour-pressure driving forces				
C.S.I.R.O.	D_r (m^3 s kg^{-1})	7.98×10^{-10}	1.73×10^{-9}	4.11×10^{-10}
schedule	D_e (K)	3659	3925	3644
Optimised	D_r (m^3 s kg^{-1})	5.76×10^{-10}	1.15×10^{-9}	8.62×10^{-10}
schedule	D_e (K)	3814	4001	4176

Table 2. Standard errors (% moisture content) from data fitting

	Yellow Stringybark	Spotted Gum	Ironbark
Moisture-content driving forces			
C.S.I.R.O. schedule	0.233	0.387	0.102
Optimised schedule	0.224	0.659	0.221
C.S.I.R.O. parameters extrapolated to optimised schedule	0.662	6.21	0.439
Vapour-pressure driving forces			
C.S.I.R.O. schedule	1.06	0.441	0.858
Optimised schedule	1.32	2.93	1.01
C.S.I.R.O. parameters extrapolated to optimised schedule	5.08	5.20	3.42

pressure driving forces, regardless of the timber species. The standard error for moisture-content driving forces is under 1% in all cases except one, while it is greater than 1% for vapour-pressure driving forces in all cases except two. The ratio of the standard errors (vapour pressure: moisture content) from the two models ranges from 1.14 for spotted gum with the C.S.I.R.O. schedule to 8.41 for ironbark with the same schedule. This ratio gives an indication of the relative fit for the models for the range of drying conditions and driving forces considered.

When developing the optimised schedules for each species, the fitted parameters from the moisture content data obtained on the C.S.I.R.O. schedule were used. The optimised schedule involved not only a different sequence of dry and wet-bulb temperatures but also higher dry-bulb (and timber) temperatures at the end of drying. In developing the optimised schedules, we implicitly assumed that the drying model was capable of extrapolation to the higher temperatures, and here we show how well this procedure worked for the drying models with both moisture-content and vapour-pressure driving forces.

The drying model with the moisture-content driving forces extrapolated the drying behaviour better than that with vapour-pressure driving forces with the exception of spotted gum where the standard errors were 6.21% for moisture-content driving forces and 5.20% with vapour-pressure driving forces. The improvements in the extrapolation ability of the moisture-content driving forces compared with vapour-pressure driving forces for both yellow stringybark (0.662% moisture content; 5.08% vapour pressure) and ironbark (0.439%; 3.42%) were substantial, with moisture-content driving forces yielding almost an order of magnitude improvement. The difference in the case of spotted gum is difficult to explain in terms of differences in physical behaviour (such as cracking) during drying, but the extrapolation ability of both driving forces was poor for this species.

These results may be due to the complexity of the moisture movement process in timber. Many workers, including Stanish et al. (1986) have suggested that movement of water vapour, free liquid water, and water which is bound to the internal structure. Hence modelling the moisture movement process by a driving force due to only one of these components (partial pressure of water vapour, for example) is only an approximation to the overall transport process. The reason why a driving force based on the total amount of moisture present (which is related to the water vapour partial pressure and the amounts of both bound and free water) should give a better fit and wider applicability is difficult to explain. It is certainly simpler to apply than a model which incorporates multiple mechanisms for the movement of water, and this feature is a great advantage when optimising the drying schedules for hardwood timber (Langrish et al. 1997).

The results for both fitting and extrapolation also suggest that the combined impact of the difference in the fitted diffusion parameters for C.S.I.R.O. and the optimised schedules is small, particularly for the approach used here where the fitted parameters from the data obtained with the C.S.I.R.O. schedules have been used to develop the optimised schedules. The most significant feature appears to be the generally poorer fit obtained using vapour-pressure driving forces for both schedules. The fitted diffusion parameters for these driving forces result in a model which not only does not fit any data set particularly well but which also does not enable the drying behaviour to be predicted well at different conditions from the C.S.I.R.O. schedule, relative to the model with moisture-content driving forces.

Conclusions

The diffusion model with moisture-content driving forces has fitted moisture content data from two sets of drying schedules applied to timber from three species of Australian hardwoods (yellow stringybark, spotted gum and ironbark) better than a model based on vapour-pressure driving forces alone. The use of moisture-content driving forces with diffusion parameters obtained from data from one drying schedule is also better in predicting the drying behaviour with another schedule than vapour-pressure driving forces for yellow stringybark and ironbark. These results may be due to the complexity of the moisture-movement process through timber, with more than one moisture-transport mechanism being active, so that the use of only one driving force for moisture movement is at best only an approximation to the true behaviour.

References

Bramhall, G. 1995: Diffusion and the drying of wood. Wood Sci. Technol. 29: 209–215

Campbell, G. S. 1980: Index of kiln drying schedules for timber dried in Australia. Commonwealth Scientific and Industrial Research Organisation Building Research Division

Doe, P. D.; Oliver, A. R.; Booker, J. D. 1994: A non-linear strain and moisture content model of variable hardwood drying schedules. Proc. 4th IUFRO International Wood Drying Conference, pp. 203–210, Rotorua, New Zealand

Langrish, T. A. G.; Brooke, A. S.; Davis, C. L.; Musch, H. E.; Barton, G. W. 1997: An improved drying schedule for Australian ironbark timber: optimisation and experimental validation. Accepted for publication in Drying Technology 15(1)

Pang, S.; Langrish, T. A. G.; Keey, R. B. 1994: Moisture movement in softwood timber at elevated temperatures. Drying Technology 12(8): 1897–1914

Simpson, W. T.; Rosen, H. N. 1981: Equilibrium moisture content of wood at high temperatures. Wood Fiber 13(3): 150–158

Stanish, M. A.; Schajer, G. S.; Kayihan, F. 1986: A mathematical model of drying for porous hygroscopic media. AIChE J 32(8): 1301–1311

Wu, Q. 1989: An investigation of some problems in drying of Tasmanian eucalypt timbers. M. Eng. Sc. thesis, Univ. Tasmania, 237 p.